Journal of Biomechanical Science and Engineering

Vol. 8, No. 1, 2013

# Compressive Deformation Analysis of Alginate-Poly(L)lysine-Alginate (APA) Microcapsule*

Kiyoshi BANDO**

**Department of Mechanical Engineering, Kansai University

3-3-35 Yamate-cho, Suita, Osaka, Japan

E-mail: bando@kansai-u.ac.jp

**Abstract**

An analysis of the compressive deformation of alginate-poly(L)lysine-alginate (APA) microcapsules by two rigid parallel plates was performed under the assumptions that the bending stiffness and permeability of the membrane were negligible. The static equilibrium equations of force for axisymmetric elastic deformation were solved using the Runge-Kutta method with the constraint of constant microcapsule volume during deformation. The constitutive laws of a neo-Hookean material and that proposed by Evans and Skalak[1] were used. The Young's modulus of the membrane was determined by an atomic force microscopy (AFM)-based technique, and a comparison with a semianalytical solution neglecting the shear stiffness of the membrane validated the present analysis method. The force–displacement curve for the compressive deformation of an APA microcapsule is calculated and compared with the experimentally measured result. A nonlinear increase in the transmural pressure with increasing displacement and the meridional and circumferential stress resultant distributions near rupture of the membrane are also shown.

***Key words***: Microcapsule, Mechanical Properties, Compression, Modeling, Membrane, Constitutive Law

## 1. Introduction

Microcapsules are widely used for various medical applications such as drug delivery, cell therapy, and artificial organs. The mechanical properties of microcapsules are of great importance not only for knowledge about the deformation capacity against mechanical stresses applied by the surrounding environment but also for designing and controlling the release of encapsulated substances via changes in the transmural pressure. There are several experimental methods for examining the mechanical properties of microcapsules and cells, such as micropipette aspiration[2], poking[3], atomic force microscopy (AFM)[4], and optical tweezers[5,6]. Another widely used technique is a compression test using two rigid parallel plates[7-14] in which the compression force and deformation of the microcapsule are monitored. The mechanical properties of the microcapsule membrane are extracted through (1) measurement of the compression force versus plate displacement curve and (2) fitting a theoretical model to the measured force–displacement curve[9,11-13]. The membrane model proposed by Feng and Yang[15] and Lardner and Pujara[16] is often used for the theoretical calculations. Feng and Yang[15] considered the deformation problem of an inflated, gas-filled elastic membrane compressed between two rigid parallel plates, and Lardner and Pujara[16] extended this model by considering a sphere filled with an incompressible fluid.

In our previous research[14], the Young's modulus of an alginate-poly(L)lysine-alginate (APA) microcapsule membrane was determined by an AFM-based technique. APA microcapsules are widely used as vehicles for the delivery of encapsulated cells[17,18]. In the present research, the force–displacement relationship is predicted by the theoretical analysis, in which the experimentally obtained Young's modulus is used as a datum of the

*Received 14 Aug., 2012 (No. 12-0326)
[DOI: 10.1299/jbse.8.40]

membrane property. The deformation analysis used here is based on the works[15,16]. The bending stiffness and permeability of the membrane are neglected, and frictionless contact between the plate and membrane is assumed, and the constitutive law of a neo-Hookean (NH) material[19] and the constitutive law proposed by Evans and Skalak[1] are applied. To verify the theoretical analysis, the calculated force–displacement curve, for which uniform and isotropic tension is assumed, is compared with the semianalytical result[14]. The calculated and experimentally measured force–displacement curves are compared, and the limitations and problems of the theoretical analysis are discussed. The increase in the transmural pressure with increasing displacement is shown, and its medical importance is addressed. The distributions of the stress resultants before membrane rupture are also demonstrated.

## 2. Theoretical analysis

Before describing the theoretical analysis, the microcapsule compression experiment[14] corresponding to the present analysis is summarized. APA microcapsules 200–300 μm in diameter were produced following the method of Okada et al.[20] The Young's modulus of the membrane $E$ was determined by applying the Hertz contact theory[21] to the results of the indentation test using AFM. A value of $E = 1.9$ MPa was obtained for an assumed Poisson's ratio $\nu$ of 0.5. Microcapsules 240 μm in diameter and 7.75 μm in thickness, confirmed with a CCD camera (CCD-IRIS, Sony Corp.) through an inverted microscope (IX-70, Olympus Corp.), were placed in a micromanipulator system (MMS-77, Shimadzu Corp.) for the compression tests. As shown in Fig.1, a microcapsule is placed between two flat silicon substrates; one substrate is connected to a manipulator and the other is adhered to a cantilever, which in turn is connected to a manipulator. The upper manipulator in Fig. 1 was driven downward (loading) and then upward (unloading) at a speed of approximately 15 μm/s, thus compressing and releasing the microcapsule. The compression was done up to approximately 40% non-dimensional displacement ( $\delta / R_0$ ), before membrane rupture occurred. Membrane rupture was observed at a non-dimensional displacement of nearly 50%. The force applied to the microcapsule was determined from the product of the cantilever deflection and stiffness.

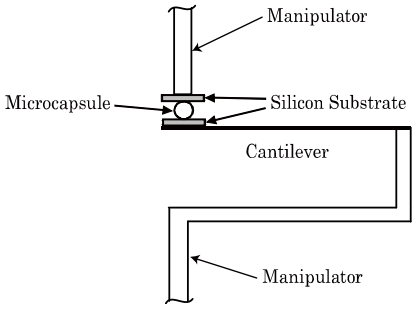


Fig.1 Micromanipulator for microcapsule compression

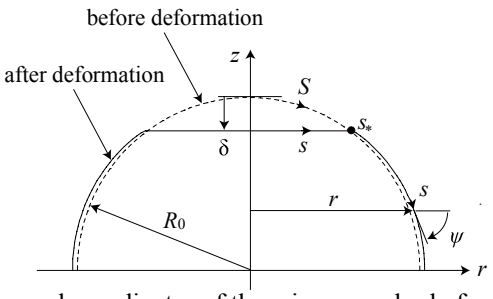


Fig.2 Geometry and coordinates of the microcapsules before and after deformation

In the calculation, $\nu$ was assumed to be 0.5 based on the following. The produced microcapsules were preserved in saline solution for a long period of time, and the compression tests were performed in the saline solution immersed state; thus, the membrane was in a fully swollen state as a polymer gel. In such a case, the mechanical behavior of the membrane can be considered to be similar to that of rubber-like materials[23,24], which have

Poisson's ratios of approximately 0.5 up to a stretch ratio of approximately 3.5[25].

The theoretical analysis of the compressive deformation of a microcapsule by two rigid parallel plates is based on the formulations[15,16]. The microcapsule is assumed to initially be a sphere with radius $R_0$, and the deformed shape is assumed to be axisymmetric. For simplicity, we can consider one hemisphere of the microcapsule. The meridional shapes of the microcapsule before and after contact with one plate are shown in Fig. 2. The cylindrical coordinate system $(r, z)$ is taken, and the meridional lengths of the initial and deformed shapes are *S* and *s*, respectively, whose origins are located on the *z*-axis. The contact region $0 \le s \le s_*$ corresponds to the initial region of $0 \le S \le S_*$.

The static equilibrium equations of force for an axisymmetric membrane with negligible bending stiffness in the meridional, tangential, and normal directions are [22]

$$\frac{dT_s}{ds} + \frac{1}{r}\frac{dr}{ds}(T_s - T_\varphi) = 0 \tag{1}$$

$$\kappa_s T_s + \kappa_\varphi T_\varphi = p_{tr} \tag{2}$$

where $T_s$ and $T_\varphi$ are the principal stress resultants in the meridional and circumferential directions, respectively; $\kappa_s$ and $\kappa_\varphi$ are the principal curvatures in the meridional and orthogonal planes, respectively; and $p_{tr}$ is the transmural pressure defined by

$$p_{tr} = p_i - p_e \tag{3}$$

where $p_i$ and $p_e$ are the uniform internal and external pressures on the membrane, respectively.

The principal stretches in the meridional and circumferential directions are, respectively,

$$\lambda_s = \frac{ds}{dS}\ ,\ \lambda_\varphi = \frac{r}{R} \tag{4}$$

where *R* is defined as the initial coordinate of *r* for the same material point. The principal curvatures are expressed by

$$\kappa_s = \frac{d\psi}{ds} = \frac{\psi'}{\lambda_s}\ ,\ \kappa_\varphi = \frac{\sin\psi}{r} \tag{5}$$

where $\psi$ is the angle between the *s*- and *r*-directions as shown in Fig. 2, and the prime indicates differentiation with respect to *S*.

The principal stress resultants of the deformed membrane are expressed as

$$T_s = T_s(\lambda_s, \lambda_\varphi)\ ,\ T_\varphi = T_\varphi(\lambda_s, \lambda_\varphi) \tag{6}$$

for which the functions $T_s$ and $T_\varphi$ depend on the strain-energy function of the material under consideration.

Based on these assignments, Eq. (1) is transformed into the following equation.

$$\lambda_s' = -\left[\frac{\partial T_s}{\partial \lambda_\varphi}\lambda_\varphi' + \frac{\lambda_s \cos\psi}{r}(T_s - T_\varphi)\right] \Big/ \frac{\partial T_s}{\partial \lambda_s} \tag{7}$$

Differentiation of the $\lambda_\varphi$ equation in Eq. (4) with respect to *S* gives

$$\lambda_\varphi' = \frac{\lambda_s \cos\psi - \lambda_\varphi \cos(S/R_0)}{R} \tag{8}$$

Substitution of Eq. (5) into Eq. (2) gives

$$\psi' = \frac{\lambda_s}{T_s}\left(p_{tr} - \frac{\sin\psi}{r}T_\varphi\right) \tag{9}$$

To obtain the deformed shape of the microcapsule, the following differential equations are used.

$$r' = \lambda_s \cos\psi \tag{10}$$

$$z' = -\lambda_s \sin\psi \tag{11}$$

The boundary conditions for this problem are

$$S = 0\text{: } \lambda_s = \lambda_\varphi = \lambda_0 \text{ and } r = 0 \tag{12}$$

$$S = S_*\text{: } (\lambda_s)_{\text{contact}} = (\lambda_s)_{\text{no-contact}},\ (\lambda_\varphi)_{\text{contact}} = (\lambda_\varphi)_{\text{no-contact}},\ \psi = 0,$$

$$(r)_{\text{contact}} = (r)_{\text{no-contact}} \text{ and } (z)_{\text{contact}} = (z)_{\text{no-contact}} \tag{13}$$

$$S = \frac{\pi}{2} R_0\text{: } \psi = \frac{\pi}{2} \tag{14}$$

where $(z)_{\text{contact}}$ in Eq. (13) is specified arbitrarily and then modified after the calculation of a deformed shape such that the equator of the microcapsule is always located at $z = 0$. Eq. (14) expresses the symmetry condition at the equator of the microcapsule.

The volume of the microcapsule is assumed to be constant during deformation under the assumption that the encapsulated fluid is an incompressible liquid and that the permeability of the membrane is neglected. This is satisfied by

$$\frac{2\pi}{3}\int_{s_*}^{s_e} r(n_r r + n_z z)ds + \frac{\pi}{3} s_*^2 (z)_{\text{contact}} = V_0 \tag{15}$$

where $s_e$ indicates the $s$ coordinate at the equator of the microcapsule, $n_r$ and $n_z$ are the $r$- and $z$-components, respectively, of the outward normal unit vector to the membrane surface, and $V_0 (= 2\pi R_0^3 / 3)$ is the initial volume. Eq. (15) is derived by applying the Gauss divergence theorem to the volumetric integral of $(\nabla \cdot \boldsymbol{x})/3$, where $\boldsymbol{x}$ is a position vector.

The applied compression force $F$ is calculated by

$$F = \pi s_*^2 p_{tr} \tag{16}$$

This equation is obtained from the force balance in the $z$-direction of the flat part of the membrane that is in contact with the plate.

We consider two constitutive laws that have commonly been used to describe the behavior of thin membranes. The neo-Hookean (NH) law[19] for rubber-like materials is expressed by

$$T_s = \frac{Eh}{3}\left(\frac{\lambda_s}{\lambda_\varphi} - \frac{1}{\lambda_s^3 \lambda_\varphi^3}\right) \tag{17}$$

where $h$ is the initial thickness of the membrane. The expression for $T_\varphi$ is obtained by interchanging the indices $s$ and $\varphi$. The second constitutive law proposed by Evans and Skalak[1] (the ES law) to model biological membranes is expressed by

$$T_s = K(\lambda_s \lambda_\varphi - 1) + \mu \frac{\lambda_s^2 - \lambda_\varphi^2}{2\lambda_s^2 \lambda_\varphi^2} \tag{18}$$

where $K$ is the area dilatation modulus and $\mu$ is the shear modulus. The relationships between these quantities and $E$ and $v$ under a small deformation plane stress assumption are as follows[12].

$$K = \frac{Eh}{2(1-v)},\ \mu = \frac{Eh}{2(1+v)} \tag{19}$$

An outline of the numerical calculation procedure is as follows:

[1] Assign a value for $S_*$.

[2] Assume values for $\lambda_0$ and $p_{tr}$.

[3] In the contact region, apply the Runge-Kutta method to Eqs. (7), (8), and (10) with $\psi = 0$. The initial conditions are given by Eq. (12).

[4] In the no-contact region, apply the Runge-Kutta method to Eqs. (7)–(11). The initial conditions are given by Eq. (13).

[5] Check the conditions expressed in Eqs. (14) and (15). If they are not satisfied, assume new values of $\lambda_0$ and $p_{tr}$ and repeat procedures [2]–[5] until the conditions are satisfied.

## 3. Results and discussion

To verify our analysis, the results obtained using the semianalytical method[14] were

compared with those calculated using the present method. In the semianalytical method, the assumption of a uniform and isotropic membrane tension enables Eq. (2) to be solved analytically with two unknown parameters that are determined numerically; only the area dilatation modulus $K$ is used in the constitutive law. Therefore, performing the present calculation with $\mu = 0$ for an ES material should yield the same result as the semianalytical method. Fig. 3 shows a comparison of the compression force versus the non-dimensional displacement results. The calculation results are in good agreement.

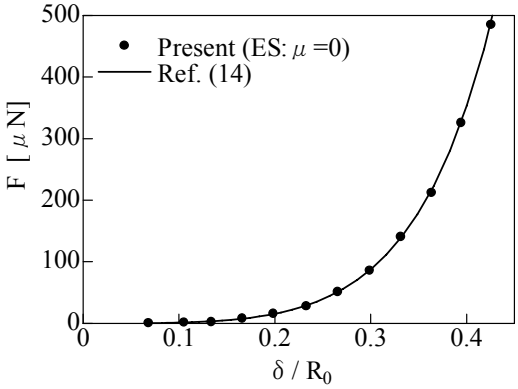


Fig.3 Comparison of the calculation results ($h$ = 7.75μm)

The force–displacement experimental results are shown in Fig. 4 where the open circles denote the loading values and the open triangles denote the unloading values. The hysteresis seen in the curve is due to the permeation of liquid across the membrane[14]. Also shown by the solid line with black circles are the calculation results for an NH material; these results are reversible for the loading–unloading process. A comparison with the experimental results reveals that the calculated force is slightly underpredicted in the small deformation region. This difference may arise from the fact that the membrane bending stiffness has an effect when the deformation is small[26]. In contrast, the calculated force is overpredicted in the large deformation region. This may be due to the fact that the membrane permeability is not accounted for in the theoretical model.[13]

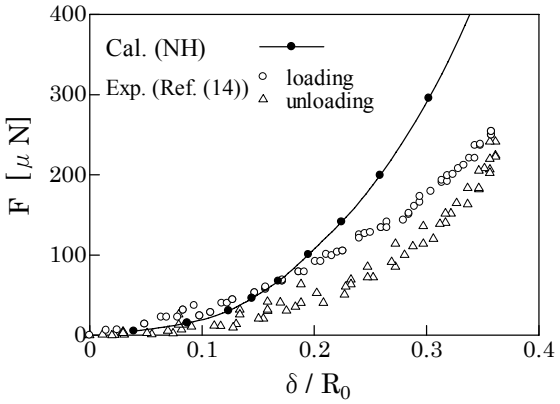


Fig.4 Comparison of calculated and experimental results

The influence of the constitutive law on the force–displacement curve is shown in Fig. 5. The calculations were performed in a non-dimensional displacement $\delta / R_0$ range smaller than 0.5 to avoid membrane rupture. The results for the NH and ES materials are coincident in the range of $\delta / R_0 < 0.25$, and the results for the NH material are smaller than those for the ES material in the range of $\delta / R_0 > 0.25$. Furthermore, the experimental results in Fig. 4 are smaller than the results for the NH material in the range of $\delta / R_0 > 0.2$. Therefore, the results for the NH material are nearer to the experimental results than the results for the ES material. In the large deformation region, a microcapsule

with an ES material membrane has a somewhat higher bulk elastic stiffness than that with an NH material membrane. The difference in the large deformation region is, in a sense, considered to be significant, when values with the same contact angle $\theta_*$ are compared. The contact angle is defined as

$$\theta_* = S_* / R_0 \tag{20}$$

The difference between the ES results in Fig. 5 and the analytical data in Fig. 3 indicates the force induced by the shear stiffness of the membrane in the ES material.

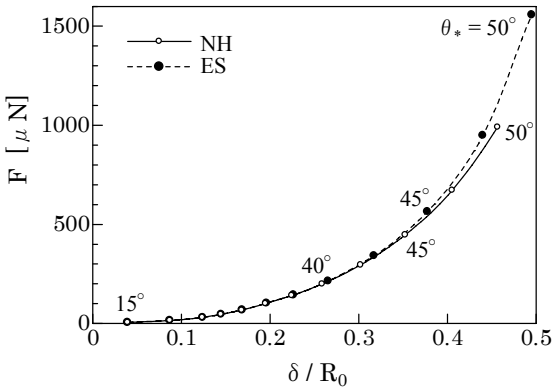


Fig.5 Comparison of the calculation results for the NH and ES materials

The transmural pressure as a function of the non-dimensional displacement for the NH and ES materials is shown in Fig. 6. The difference between the NH and ES materials follows a similar trend to that in Fig. 5. The transmural pressure is important not only for preservation of the microcapsule shape but also for the release of the encapsulated solutions. The volume flux of the liquid across the membrane is calculated from the product of the transmural pressure and the permeability of the membrane[13]. Therefore, the results in Fig. 6 are crucial for controlling drug release in drug delivery systems.

The deformed shapes of the NH and ES material microcapsules for different contact angles $\theta_*$ are shown in Fig. 7. As was evident in Fig. 5, for the same contact angle $\theta_*$, the displacement of the ES material is larger than that of the NH material in the large displacement region. Therefore, the deformation of the ES material (shown by the broken lines) in Fig. 7 is larger than that of the NH material (shown by the solid lines).

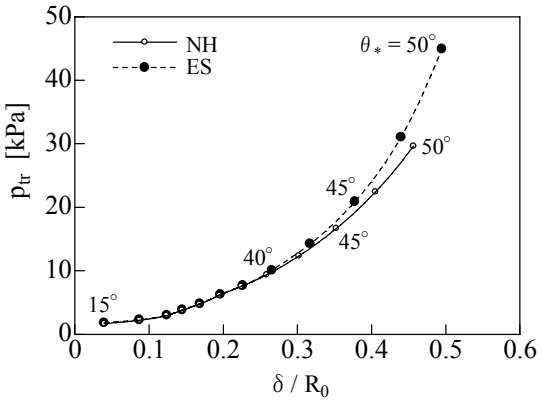


Fig.6 Increase in transmural pressure with increasing non-dimensional displacement

In Fig. 8, the distributions of the principal stress resultants $T_s$ and $T_\varphi$ are shown for contact angles of $\theta_* = 40^\circ$ and $50^\circ$. The points indicated by the black circles are the boundary points between the contact and no-contact regions. The stress resultant $T_\varphi$ is always larger than $T_s$ for both the NH and ES materials, and both stress resultants for the ES material are always larger than those for the NH material because the deformation of the

ES material is larger than the NH material when both materials are compared at the same contact angle $\theta_*$, as shown in Fig. 7. Negative tensions in the contact region are seen at $\theta_* = 40^\circ$ for both the NH and ES materials and at $\theta_* = 50^\circ$ for only the NH material. Buckling may take place in the negative tension region; however, the $\psi = 0$ constraint over the contact region prevents this. At a contact angle of $\theta_* = 50^\circ$, where the non-dimensional displacement is close to 0.5 as shown in Fig. 5, the state of the membrane tension is that just before rupture. The tensions are a maximum at the equator of the capsule and rupture will take place there. This prediction is consistent with the experimental observations[9]. As shown in Fig. 5, the non-dimensional displacement at a contact angle of $\theta_* = 50^\circ$ for the ES material is $\delta / R_0 = 0.495$, which is close to the state of membrane rupture. The calculated distributions of the tensions $T_s$ and $T_\varphi$ for the NH material at $\delta / R_0 = 0.495$ (not shown here) are smaller than those for the ES material, showing the same trend as the right-hand side figure in Fig. 8. Therefore, the NH material is considered to have a higher resistance against membrane rupture than the ES material.

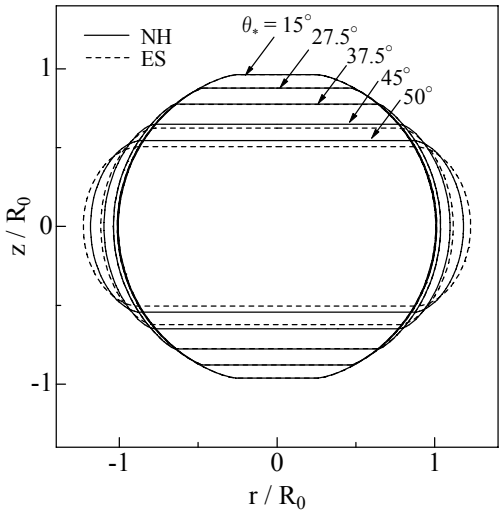


Fig.7 Shapes of the deformed microcapsules for the NH and ES materials

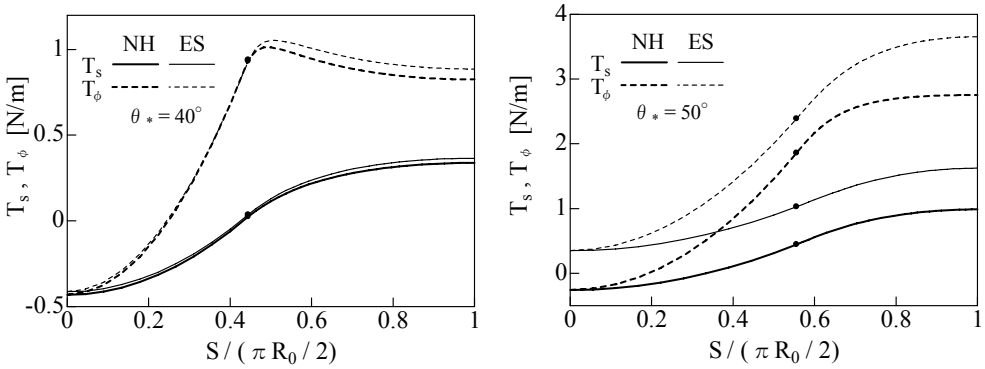


Fig.8 Distributions of the tensile stress resultants

The relationship between $\lambda_s$ and $\varepsilon_s$ (strain) in the small deformation range is $\varepsilon_s = \lambda_s - 1$, and a similar relationship holds for $\lambda_\varphi$ and $\varepsilon_\varphi$. The small deformation assumption ignores the second- and higher-order terms of $\varepsilon_s$ and $\varepsilon_\varphi$. Therefore, the application range of Eq. (19), which assumes small deformation, is considered to be the range for which the differences of $\lambda_s$ and $\lambda_\varphi$ from unity are smaller than 0.1. Calculation results (not shown here) indicate that $\lambda_\varphi$ becomes slightly larger than 1.1 in the no-contact

region when the contact angle exceeds $\theta_* = 45°$. Thus, the calculation results in Figs. 5–8 for the ES material are valid in the range where the contact angle is smaller than $45°$ and those that exceed the contact angle of $45°$ involve errors due to second-order terms of the strain. However, according to Carin et al.[11], a larger force is needed for the ES material than for the NH material for the same compression. Carin et al.[11] did not apply the small deformation assumption in Eq. (19) but obtained the same force–displacement relationship as that shown in Fig. 5. Therefore, Eq. (19) may be used in the finite deformation region. In this study, only the value of $K/\mu = 3$ was examined, which is derived from Eq. (19) with $\nu = 0.5$. Carin et al.[11] varied the value of $K/\mu$ from 0.1 to 3 and calculated the corresponding force–displacement curves. This variation is necessary to solve the inverse problem for extracting mechanical parameters from the fitting of the calculated and measured force–displacement curves.

## 4. Conclusions

An analysis of the compressive deformation of APA microcapsules by two rigid parallel plates was performed for NH and ES material membranes. The calculated compression force due to the plate displacement was smaller than the experimentally measured force in the small deformation region and was larger in the large deformation region. The difference between the predicted and experimental results can be decreased by incorporating the bending stiffness and permeability of the membrane into the theoretical model. The calculated results for the NH and ES material constitutive laws were in good agreement in the small and medium deformation regions, but a difference appeared in the large deformation region. A theoretical prediction of the resistance against membrane rupture is therefore dependent on the selection of the constitutive law of the membrane. Judging from the calculation results, the NH material has a somewhat higher resistance against membrane rupture than the ES material. The calculation of the increase in transmural pressure with increasing compressive deformation is an important result for the application of microcapsules as a drug delivery system because the transmural pressure is directly related to drug release across the membrane.

In calculations[9,11-13] similar to the present study, the mechanical parameters of the membrane were determined such that the calculated force–displacement curve fitted well with experimentally measured curve. The validity of such a method in determining the mechanical parameters should be examined. In the present study, the Young's modulus was determined experimentally using AFM, and Poisson's ratio was determined from a consideration of the compressive experiment in which the fully swollen state of the polymer gel membrane can be assumed. The degree of coincidence between the calculated and measured force–displacement curves was shown to be a good measure for judging the validity of the parameter-fitting method. The problem of the present study in determining the Young's modulus is that the constitutive equation of the material used in the AFM experiment, i.e., that of a three-dimensional homogeneous isotropic Hookean material, is different from that used in the compressive experiment, i.e., that of an NH or ES material.

## References

(1) Evans, E.A. and Skalak, R., *Mechanics and Thermodynamics of Biomembranes*, (1980), CRC Press.
(2) Hochmuth, R.M., Micropipette aspiration of living cells, *Journal of Biomechanics*, Vol.33(2000), pp.15-22.
(3) Goldmann, W.H., Mechanical manipulation of animal cells: cell indentation, *Biotechnology Letters*, Vol.22(2000), pp.431-435.
(4) Radmacher, M., Measuring the elastic properties of living cells by the atomic force microscope, *Method in Cell Biology* (Eds. Jena, B.P. and Horber, H.J.K.), Vol.68 (2002), pp.67-90, Elsevier.
(5) Hénon, S., Lenormand, G., Richert, A. and Gallet, F., A new determination of the shear modulus of the human erythrocyte membrane using optical tweezers, *Biophysical Journal*, Vol.76(1999), pp.1145-1151.

(6) Helfer, E., Harlepp, S., Bourdieu, L., Robert, J., MacKintosh, F.C. and Chatenay, D., Microrheology of biopolymer-membrane complexes, *Physical Review Letters*, Vol.85(2000), pp.457-460.
(7) Hiramoto, Y., Mechanical properties of sea urchin eggs, *Experimental Cell Research*, Vol.32(1963), pp.59-75.
(8) Yoneda, M., Tension at the surface of sea urchin eggs on the basis of 'liquid – drop' concept, *Advances in Biophysics*, Vol.4(1973), pp.153- 190.
(9) Liu, K.K., Williams, D.R. and Briscoe, B.J., Compressive deformation of a single microcapsule, *Physical Review E*, Vol.54(1996), pp.6673-6680.
(10) Zhang, Z., Blewett, J.M. and Thomas, C.R., Modelling the effect of osmolality on the bursting strength of yeast cells, *Journal of Biotechnology*, Vol.71(1999), pp.17 – 24.
(11) Carin, M., Barthès-Biesel, D., Edwards-Lévy,F., Postel, C. and Andrei, D.C., Compression of biocompatible liquid-filled HSA-alginate capsules: Determination of the membrane mechanical properties, *Biotechnology and Bioengineering*, Vol.82(2003), pp.207- 212.
(12) Risso, F. and Carin, M., Compression of a capsule: Mechanical laws of membranes with negligible bending stiffness, *Physical Review E*, Vol.69(2004), 061601-1-7.
(13) Wang, C.X., Wang, L. and Thomas, C.R., Modelling the mechanical properties of single suspension-cultured tomato cells, *Annals of Botany*, Vol.93(2004), pp.443-453.
(14) Bando, K., Ohba, K. and Oiso, Y., Deformation analysis of microcapsules compressed by two rigid parallel plates, *Journal of Biorheology*, (to be published).
(15) Feng, W.W. and Yang, W.-H., On the contact problem of an inflated spherical nonlinear membrane, *Journal of Applied Mechanics*, Vol.41 (1973), pp.209-214.
(16) Lardner, T.J. and Pujara, P., Compression of spherical cells, *Mechanics Today* (Ed. Nemat - Nasser, S.), Vol.5 (1980), pp.161-176, Pergamon Press.
(17) Tai, I.T. and Sun, A.M., Microencapsulation of recombinant cells: a new delivery system for gene therapy, *FASEB Journal*, Vol.7(1993), pp.1061-1069.
(18) Joki, T., Machluf, M., Atala, A., Zhu, J., Seyfried, N.T., Dunn, I.F., Abe, T., Carroll, R.S. and Black, P.M., Continuous release of endostatin from microencapsulated engineered cells for tumor therapy, *Nature Biotechnology*, Vol.19(2001), pp.35-39.
(19) Treloar, L.R.G., *The Physics of Rubber Elasticity*, (1975), Oxford University Press.
(20) Okada, N., Miyamoto, H., Yoshioka, T., Katsume, A., Saito, H., Yorozu, K., Ueda, O., Itoh, N., Mizuguchi, H., Nakagawa, S., Ohsugi, Y. and Mayumi, T., Cytomedical therapy for IgG1 plasmacytosis in human interleukin-6 transgenic mice using hybridoma cells microencapsulated in alginate-poly(L)lysine-alginate membrane, *Biochimica et Biophysica Acta*, Vol.1360(1997), pp.53-63.
(21) Sneddon, I.N., The relation between load and penetration in the axisymmetric Boussinesq problem for a punch of arbitrary profile, *International Journal of Engineering Science*, Vol.3(1965), pp.47-57.
(22) Flügge, W., *Stresses in Shells*, (1973), Springer.
(23) Anseth, K.S., Bowman, C.N. and Brannon-Peppas, L., Mechanical properties of hydrogels and their experimental determination, *Biomaterials*, Vol.17(1996), pp.1647-1657.
(24) Ahearne, M., Yang, Y., Haj, A.J.E., Then, K.Y. and Liu, K.-K., Characterizing the viscoelastic properties of thin hydrogel-based constructs for tissue engineering applications, *Journal of The Royal Society Interface*, Vol.2(2005), pp.455-463.
(25) Urayama, K., Takigawa, T. and Masuda, T., Poisson's ratio of poly(vinyl alcohol) gels, *Macromolecules*, Vol.26(1993), pp.3092-3096.
(26) Taber, L.A., Compression of fluid-filled spherical shells by rigid indenters, *Journal of Applied Mechanics*, Vol.50(1983), pp.717-722.